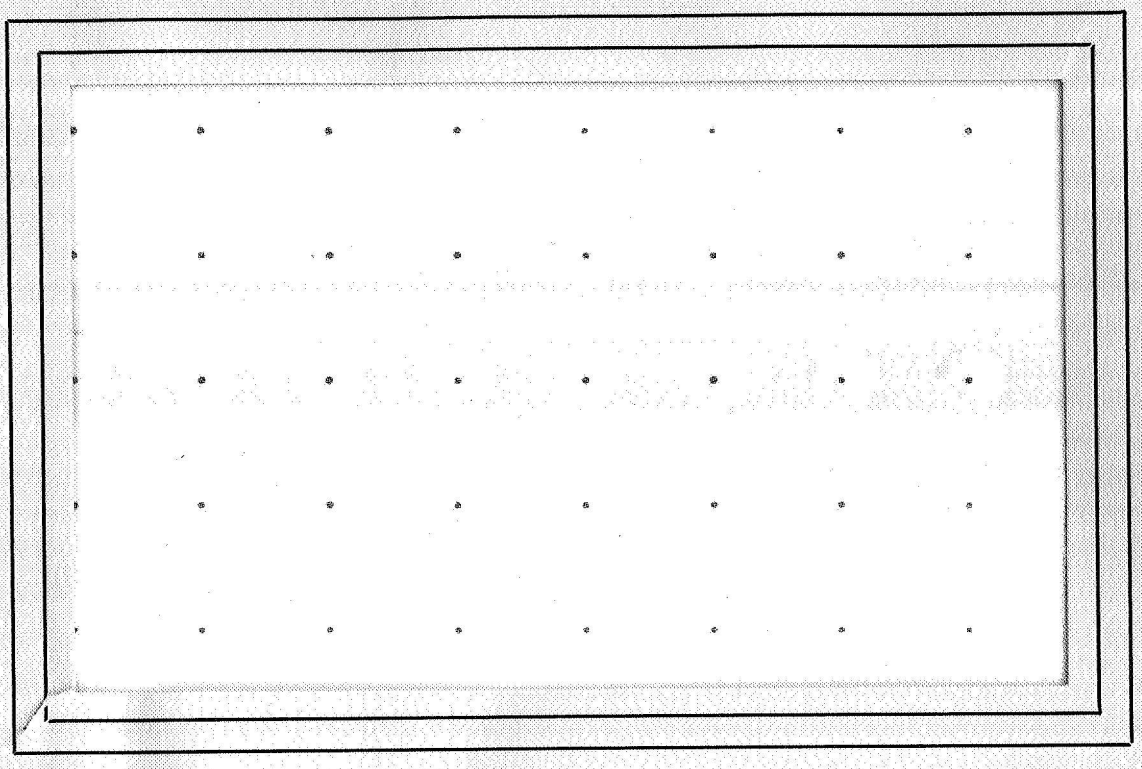

LABORATORY FOR NUCLEAR SCIENCE

MASSSACHUSETTS INSTITUTE OF TECHNOLOGY

CAMBRIDGE, MASSACHUSETTS

LOW ENERGY ELECTRONS IN THE MAGNETOSPHERE AS OBSERVED BY OGO-1 AND OGO-3

by

Vytenis M. Vasyliunas

Laboratory for Nuclear Science and Physics Department
Massachusetts Institute of Technology
Cambridge, Massachusetts

Presented at the Summer Institute - Physics of the Magnetosphere, June 19-28, 1967, Boston College, Chestnut Hill, Massachusetts.

To be published in Physics of the Magnetosphere, edited by R. L. Carovillano, J. F. McClay and H. R. Radoski (D. Reidel Publishing Company, Dordrecht).

Although the first observation of low energy (a few hundred ev to a few kev) electrons in the magnetosphere dates back to the early days of space exploration (Gringauz et al., 1960), detailed studies of these particles have been undertaken only in the last few years. The launch of Vela 2 in July 1964 initiated the first extensive survey of the low energy electron population. Observations with electrostatic analyzers aboard the Vela satellites (Bame et al., 1966, 1967) showed that the low energy electrons form part of a plasma sheet stretching across the tail of the magnetosphere, with a broad, quasi-thermal, non-Maxwellian energy spectrum peaked in the vicinity of 1 kev. However, the orbits of the Vela satellites are circular and hence all their observations are confined to geocentric radial distances near 17 Re (earth radii). A complementary survey of low energy electrons, to study their distribution in radial distance, first became possible a few months after Vela 2, with the launch of OGO-1 into a highly eccentric orbit on September 5, 1964; this satellite carries, among its many experiments, a Faraday cup to detect electrons in the 100 ev - 2 kev range. I shall be reporting results obtained with this detector and a similar one flown two years later on OGO-3.

How the modulated Faraday cup works has already been discussed at this meeting by Dr. Binsack and I shall not repeat his description. The OGO-1 instrument measures electron fluxes in four overlapping energy windows covering the range 125-2000 ev; the OGO-3 instrument has a somewhat wider energy range, extending down to 40 ev. Both have relatively high time resolution: the currents in all four energy windows are measured every 9.216 seconds in OGO-1, every 4.608 seconds in OGO-3.

The geocentric distances at apogee of OGO-1 and OGO-3 are 24.4 and 20.2 Re, respectively; both have highly eccentric orbits, with inclinations near 31° (initially), and initial apogee directions toward the magnetospheric tail on the dusk (evening) side of the earth. Observations within the magnetosphere that have been analyzed to date refer primarily to the local time range approximately between 17 and 22 hours. An extensive description of the instrumentation, orbits, methods of analysis, etc. has been given elsewhere (Vasyliunas, 1968).

In this paper I will first briefly describe the general configuration of the plasma sheet and then discuss in some detail the termination of the plasma sheet on the earthward side and its relation to magnetic bay activity.

Figure 1 shows a sketch of the low energy electron distribution in the equatorial region of the magnetosphere, as inferred from Vela and OGO observations. The dominant feature is the plasma sheet, observed as a region of greatly enhanced low energy electron fluxes; the electron population within it is characterized typically by density $\approx 0.3 - 1$ cm^{-3}, mean energy $\approx 0.5 - 2$ kev and energy density ≈ 1 kev cm^{-3}, equal to the energy density of a $\approx 20\gamma$ magnetic field (see Bame et al., 1967, and Vasyliunas, 1968, for a detailed discussion of these quantities). The plasma sheet extends across the entire tail from the dusk to the dawn boundaries of the magnetosphere, as first shown by the Vela observations. On the dusk side the OGO satellites have mapped its extent in radial distance. Going outward from the earth, the plasma sheet is sharply bounded by the magnetopause. Going inward toward the earth, the plasma sheet is also observed to have a sharp, well-defined termination;

this inner boundary of the plasma sheet, as I shall call it, inside of which only very weak or no low energy electron fluxes are found, occurs throughout the evening sector at a radial distance (near the equatorial plane) that is typically 11 ± 1 Re; this is close to, perhaps somewhat farther than, the outer boundary of the high energy trapped radiation belt, as inferred from observations of 40 kev and higher energy electrons (Frank, 1965; Serlemitsos, 1966). Finally, in local time the plasma sheet extends over the entire range so far studied in the OGO data, from 22 hours (where OGO-1 observations overlap those of Vela) to less than 17 hours; the plasma sheet is not confined to the tail but extends past the dusk meridian into the dayside magnetosphere. Wedged between the flaring-out magnetopause on one side and the nearly circular inner boundary on the other, the plasma sheet becomes very narrow indeed as one moves to earlier local times, but nevertheless it is clearly present (it has already been observed by OGO-3 at 60° from the subsolar point, where its radial extent is only 1 Re).

Figure 1 is a view in the equatorial plane; a sketch of the electron distribution in a late evening meridian plane (along the line CC' in Figure 1) is shown in Figure 2. As established first by Vela at a radial distance of 17 Re and subsequently confirmed by OGO-3 over a wide range of distances, the plasma sheet is confined to the equatorial region, within several Re above and below the magnetic neutral sheet in the tail and within a similar distance of (roughly) the geomagnetic equator on the dusk side. In particular, OGO-3 does not detect a plasma sheet next to the magnetopause at higher latitudes, contrary to the suggestion of Dessler and Juday (1965); the plasma sheet appears to be a phenomenon

purely of the equatorial region of the magnetosphere. The inner boundary has been traced by OGO-3 up to the highest latitudes ($\approx 40^{\circ}$) explored by it, and appears to have the shape, very roughly, of a dipolar field line. There is as yet little data on the electron distribution at high latitudes ($> 60^{\circ}$); what there is, the single traversal of this region by Mars 1 (Gringauz et al., 1964), suggests that the plasma sheet comes down near the auroral zones, in the horn-like fashion shown.

Summarizing, the spatial extent of the plasma sheet can be described in terms of three boundaries. First, the plasma sheet is bounded on the outside laterally, by the magnetopause. Second, it is bounded on top and bottom, roughly by planes parallel to the magnetic neutral sheet. And third, it is also bounded on the inside, roughly by a magnetic shell that crosses the equator at a distance of $\approx$ 11 Re. If the first boundary is obvious and the second had been theoretically predicted (Axford et al., 1965; Dessler and Juday, 1965), no one to my knowledge had predicted the third, the large apparent "hole" within the low energy electron population. The rest of this paper will be largely concerned with this unexpected inner boundary and some even more unexpected features of it.

Figure 3 shows a typical example of OGO-1 observations during an inbound pass near the dusk meridian. Plotted are the currents in the four energy windows as functions of time, with the lowest energy at the bottom of the figure and the highest at the top; the radial distance and the sun-earth-probe angle are indicated. The projection of the corresponding orbit on the geomagnetic and solar magnetospheric meridian planes is given in Figure 4; typical of most of the OGO-1 orbits during this period, the inbound pass begins somewhat high but soon comes down

and stays close to both the geomagnetic and the solar magnetospheric equatorial planes. From the beginning of the pass until the data gap near 19 Re, the satellite is in the magnetosheath, as identified by a proton detector; the highly variable fluxes confined to the lowest one or two energy channels are typical of the magnetosheath electron population, indicating that one is observing merely the high energy tail of a distribution whose peak lies below 100 ev (Vasyliunas, 1966). Somewhere within the data gap the satellite crosses into the magnetosphere. As it approaches the equatorial region (cf. Figure 4), at a distance of 16.4 Re it encounters the intense fluxes typical of the plasma sheet. From 13.6 to 11 Re the strongest fluxes are observed in the two highest energy channels, indicating a typical plasma sheet spectrum with a peak somewhere between 500 and 1000 ev. Then, the onset of the rapid changes at 11 Re marks the inner boundary of the plasma sheet. Note that the highest energy flux decreases first, then the next highest; in the two lowest energy channels the fluxes actually first increase and then decrease to the background level. In other words, as one crosses the inner boundary, moving toward the earth, the position of the peak in the electron energy spectrum shifts rapidly to lower energies. This behavior is invariably observed on every crossing of the inner boundary and is perhaps its most unexpected feature; naively one would have thought that in approaching the energetic trapped radiation belts the plasma sheet electrons would shift upward in energy and merge with the trapped particle population.

Inside of the inner boundary only very weak or no electron fluxes are observed; in Figure 3 from 10 to 5.6 Re the signals in all four

channels are at background level. (Note: the baselines in the figure represent the telemetry zero; the background signal is half a unit or so above it, primarily due to the non-linear electronics). Beginning at 5.6 Re the signals drop below the background level to zero; this effect is always observed at distances of 4-6 Re whenever data is available and marks the entry of the satellite into the plasmasphere (not to be confused with the plasma sheet!), the very high density ($n > 10^3$ cm^{-3}) region near the earth that has already been extensively studied by various techniques (Taylor et al., 1965; Carpenter, 1966; Angerami and Carpenter, 1966); secondary electrons arising from these very high ion densities force the instrument into a peculiar mode of operation (see Binsack, 1967, and Vasyliunas, 1968, for further discussion).

As illustrated by this example, five distinct regions can be identified from the OGO-1 data near the equatorial plane: (1) the magnetosheath, (2) the plasma sheet, (3) the thin "boundary layer" at the inner edge of the plasma sheet, within which the electron fluxes decrease from the plasma sheet level to unobservable values, (4) the region on the earthward side of the plasma sheet, within which electron fluxes are undetectable with the OGO-1 instrument, (5) the plasmasphere, within which the instrument response is dominated by the dense positive ion effects and no useful electron observations can be made. Figure 5 summarizes all the OGO-1 observations during the fall of 1964 in terms of these five regions: all portions of the orbits for which data are available (excluding observations near and beyond the bow shock) are shown projected on the solar magnetospheric XY (equatorial) plane, with the type of line (thick, thin, dotted, etc.) indicating to which region

electrons observed at a given location are ascribed (blank spaces and gaps, let me emphasize, represent lack of data, not lack of electrons; the OGO-1 data coverage is unfortunately far from complete). The general extent of the plasma sheet — its persistence over the entire local time range scanned and its confinement between the magnetopause and an inner boundary — is quite apparent. But it is also apparent that the position of the inner boundary is not fixed but varies over a considerable range of radial distances, from 12 to 5.5 Re. Furthermore, this variability is quite irregular; the plasma sheet may extend to less than 8 Re on one orbit and to only 11 Re on both the preceding and following orbits; there are even cases of multiple appearances and disappearances of the plasma sheet within one orbit, i.e. multiple crossings of the inner boundary. These facts strongly suggest that this variability reflects true temporal changes in the position of the plasma sheet, rather than some purely spatial variation such as a local time dependence.

If, then, the inner edge of the plasma sheet can be displaced from 11 to 6 Re, the question immediately arises whether any geomagnetic effects occur in association with the appearance of intense low energy electron fluxes at such close distances. The first possibility that comes to mind, that close distances of the inner boundary all occur during magnetic storms, turns out to be false; there is, in fact, at least one case of a close-in boundary during one of the 10 quiet days of the month. A plot of the inner boundary positions against Kp, the standard procedure in such a study, produces only the standard scatter diagram, with some indication of a possible weak trend for closer distances to occur during times of higher Kp (it should be noted that of 21 cases

available 16 have Kp values of 2^- or less and none have Kp greater than 4^+, reflecting the very low general level of geomagnetic activity near solar minimum).

J. P. Heppner (private communication) first suggested a search for an association between the close-in boundary positions and the occurrence of bay activity in the auroral zones, particularly at observatories near the same local time as the satellite; Heppner and co-workers (Heppner, 1965; Heppner et al., 1967) have already established, using OGO-1 magnetometer observations, that the sudden onset of a bay in the auroral zone near some meridian is accompanied by changes of the magnetic field in the distant magnetosphere near the same meridian. Accordingly, I examined magnetograms from a number of auroral zone stations, in particular College (Alaska), Fort Churchill (Canada), Kiruna (Sweden), Dixon Island and Cape Chelyuskin (Northern Siberia), for times of all the OGO-1 inbound passes through the magnetosphere in 1964 for which data was available. The results fully confirm Heppner's hypothesis: in every case where the plasma sheet extends to distances < 9 Re, there is clearly identifiable bay activity; in every case where the plasma sheet terminates at its "normal" distance of $\approx$ 10-12 Re, the auroral zone magnetic field is quiet. The observations are summarized in Figure 6, which shows the radial distances of inner boundary crossings plotted against magnetic local time and identified by the occurrence or non-occurrence of bays. There clearly appears to be a one-to-one correspondence between the two phenomena: magnetic bays are associated with the extension of the plasma sheet inward several Re from its quiet-time boundary.

Let me illustrate this correlation with three examples, taken from three consecutive orbits:

Figure 7 shows the OGO-1 electron observations and the simultaneous magnetograms from Fort Churchill and College for the October 11-12, 1964 inbound pass. At the beginning of the pass the satellite is descending from moderately high latitudes and first enters the plasma sheet at a distance of approximately 16.6 Re. Between 9.6 and 8.4 Re the electron fluxes decrease to background level, beginning with the highest energy channel; except for the "spike" at 8.6 Re (0636 U.T.), this looks in all respects like a normal crossing of the inner boundary, such as that in Figure 3, and one would have expected the fluxes to remain at background level for the rest of the pass down to $\approx$ 4 Re. Instead, at 0645 U.T. appreciable electron fluxes suddenly reappear; for the next 35 minutes the electron fluxes, although highly fluctuating, on the average increase and shift to higher energies, i.e. the typical behavior while crossing the inner boundary but now in reverse sequence; then at about 0720 U.T. the fluxes "settle down" to typical plasma sheet levels (but more intense than those earlier in the orbit) continuing to the end of data coverage at 0805 U.T. (at a distance of 6 Re).

A look at the magnetograms at once clarifies this complex sequence. Conditions in the auroral zone are very quiet from the beginning of the pass until 0640 U.T., with a slight enhancement of activity at Fort Churchill beginning about 0530. Then, at 0641 U.T., about three minutes before the first appearance of the unusual electron fluxes at the satellite, a negative bay begins with a very sharp onset at Fort Churchill, followed about 12 minutes later by the start of a positive bay at College; bay

activity then continues past the time of perigee. This example strongly suggests that not only is the presence of plasma sheet electrons at close distances associated with the occurrence of a magnetic bay but also the first appearance of those electrons occurs close to the time of the sudden onset of the bay. (It should be pointed out that at the time of onset the satellite and College are nearly on the same meridian, about 3 hours west of midnight, while Fort Churchill is 1 hour east of midnight, yet the closest time coincidence is between the satellite and Fort Churchill, the station showing the earliest and sharpest onset, in spite of the 4 hour separation in local time).

As the next example, Figure 8 shows the electron data together with Kiruna and Dixon Island magnetograms for the October 14, 1964 inbound pass, only 64 hours later than Figure 7 and at nearly the same local time and the same magnetic latitude; the behavior of both the electrons and the magnetic field is, nevertheless, entirely different. A completely "normal" inner boundary crossing at 10 Re, with fluxes in all channels then staying at background level for the (admittedly somewhat short) remainder of data coverage, is accompanied by absolute quiet in the auroral zone. There only is a small negative H excursion at Dixon Island somewhat earlier (around 1900 U.T.) which, interestingly, coincides approximately with an increase in electron flux near 1845 U.T.

Finally, Figure 9 shows the next inbound pass, October 17, 1964, with magnetograms from College, Cape Chelyuskin, and Dixon Island. The plasma sheet is in this case observed continuously down to a distance of 6 Re and, indeed, there is marked bay activity throughout most of the pass: a negative bay at College, a positive bay at Dixon Island, and an

"intermediate" bay that starts positive and turns negative, with a large excursion in the vertical component, at Cape Chelyuskin (which thus is probably near the dividing line between positive and negative bays [cf. Sugiura and Heppner, 1965, pp. 41-45]).

Two additional points about this example should be noted. First, the detailed structure of the inner boundary is more complicated than in the typical quiet-time case shown in Figure 3, with a well-marked second peak in the flux vs. radius curve (near 5.6 Re); I shall be saying more about this later on. Second, no unusual change in the character of the observations can be seen at a distance corresponding to the quiet-time inner boundary, 10-11 Re. Now the appearance of intense fluxes of a few hundred ev to a few kev electrons at unusually close distances can be explained in two ways: either these electrons were brought in from the outside, i.e. the plasma sheet was actually displaced inward, or else they were locally accelerated from very low energies into the detector's energy range. In the latter case, however, one would still expect a change in the electron energy spectrum at the normal position of the inner boundary, now separating the plasma sheet from the locally accelerated electrons, since there does not seem to be any reason why the spectra of these two different populations should be identical. But, as just noted, no such change is apparent in Figure 9, nor in any of the other available bay-related observations. This, then suggests that the appearance of plasma sheet electrons at close distances during magnetic bays results from a gross inward motion of the plasma. Returning to the example of Figure 7, the average radial speed of this motion can be roughly estimated by assuming that the plasma sheet is displaced from

10 to about 6 Re during the period of fluctuating fluxes, 0645 to 0720 U.T. (the observed upward shift of the spectrum during this period certainly suggests that the boundary of the plasma sheet is passing over the satellite; the fluctuations may reflect a non-steady, oscillatory, component of the motion that may be due to the inductive effects recently discussed by Cladis, 1967). This average speed then is $\approx$ 4 Re/35 min = 12 km/sec. The east-to-west electric field implied by this inward motion, assuming a magnetic field of 20γ, is $\approx$ 2.4 x 19^{-4} volts/m. If this field is assumed to exist across the entire magnetospheric tail (width $\approx$ 2 x 10^5 km), the potential drop across the tail (which then also exists across the polar cap) is $\approx$ 48 kev, in good agreement with the bay-time polar cap potential drop of 30-50 kev quoted by Axford et al. (1965) and Axford (1966).

To summarize, the OGO-1 observations show that the spatial distribution of low energy electrons undergoes a marked change at times of magnetic bays: the intense electron fluxes of the plasma sheet, which during quiet times are found only beyond a distance of 10-12 Re in the equatorial plane, during bays extend to distances as close as 5.5-6 Re. This change is most simply interpreted as the result of an inward motion of the plasma that appears to start nearly simultaneously with the onset of the bay; the one estimate of the speed of this motion that could be made is consistent with present ideas about the polar cap electric fields. A schematic illustration of what happens to the plasma sheet during a bay is given in Figure 10.

It is now of interest to go back to the data in Figure 5 and replot it, omitting observations made during periods of bay activity, so as to

obtain a picture of the electron distribution during quiet times. The result is shown in Figure 11; as can now be seen, in the absence of bay activity the inner boundary of the plasma sheet appears to be a relatively smooth and well-defined surface over the entire local time range covered in this study.

The last topic I shall discuss is the detailed local structure of the inner boundary. The most characteristic feature of the inner boundary is the rapid downward shift of the peak in the energy spectrum with decreasing radial distance, as mentioned already in discussing Figure 3. To study this phenomenon in a more quantitative way, the electron density N, energy density U (proportional to the electron pressure), and position of the peak in the differential energy spectrum E_o were estimated as functions of radial distance, starting deep within the plasma sheet and continuing inward for as long as the measured fluxes were above the background level, for a number of inner boundary crossings; these quantities were calculated by fitting an assumed functional form of the electron distribution function, representing a broadly peaked thermal distribution with a power law high energy tail, to the measured currents in the four energy windows of the detector (for a detailed description of the method and the assumed functional form see Vasyliunas, 1968). A typical example of the inner boundary structure thus obtained, for a geomagnetically quiet period (i.e. no bays), is shown in Figure 12. The energy E_o rapidly decreases going inward across the boundary, in agreement with the earlier qualitative inference. The density, however, is nearly constant and in fact slightly increases; the energy density decreases approximately exponentially with decreasing distance, as indicated by the solid line

which represents U $\sim$ exp (distance/0.4 Re), i.e. a factor of 10 decrease in 1 Re. The inner boundary thus is not the disappearance of low energy electrons that it at first sight appears to be but a shift of the electrons to still lower energies, below the range of the detector; at the inner edge of the plasma sheet there is a steep electron pressure gradient, directed outward from the earth, but only a weak density gradient that may be directed inward. The absence of a strong radial density gradient, it should be noted, is in agreement with the observation that the densities ($\approx$ 1 cm^{-3}) found within the plasma sheet are comparable with the densities at distances 5-7 Re, immediately outside the plasmasphere, deduced by whistler techniques (Carpenter, 1966 ; Angerami and Carpenter, 1966).

Turning now to the structure of the inner boundary when it is found at much closer distances, during periods of magnetic bay activity, I already drew attention in discussing the example of Figure 9 to the occurrence of a second peak in the flux vs. radius curve. In a single example such a local peak might be interpreted as merely a temporal fluctuation in the flux. This feature, however, is found in all the cases studied, indicating that it most probably represents a true spatial variation; in a typical inbound crossing of the inner boundary when it is at close distance, the measured flux first decreases rapidly (as it does during quiet times), then increases again, and finally decreases to background level. This is illustrated in Figure 13, which shows the measured signals as a function of distance for a number of inbound passes; for simplicity only two of the four energy channels, the highest and the lowest, are shown. The top four examples come from periods of bay activity; the fifth comes from a time at the end of a magnetic storm but with no identifiable bays;

the bottom two come from quiet periods. The existence of two maxima in at least one of the two energy ranges shown is quite clear for all the bay cases; in the 11/2/64 curve the flux of the higher energy electrons decreases to background at the normal position of the inner boundary, 11 Re, but the low energy electrons linger down to 7 Re, possibly a storm effect; and there is a suggestion of a small peak in the low energy electron flux inside of the inner boundary in one of the two quiet-time examples.

The variation of E_o, N, and U across the inner boundary during a bay is illustrated by the example in Figure 14. As can be seen, E_o first decreases rapidly, then increases to about half of the value it had within the plasma sheet, and finally decreases again. The density N now appreciably increases as E_o decreases, then decreases as E_o increases, and remains at about a constant value as E_o decreases again. The energy density U, however, still has the same simple structure it had in Figure 12: a monotonic, approximately exponential decrease with decreasing distance at a rate which is apparently slightly slower than that in Figure 12 (the solid line in Figure 14 represents the same rate of decrease as in Figure 12, while the dashed line represents $U \sim \exp$ (distance/0.6 Re), a factor of 10 in 1.4 Re). This behavior of the three quantities is confirmed by another example, Figure 15 (the solid and dashed lines represent the same rates as in Figure 14).

To summarize, during quiet times the inner boundary of the plasma sheet, located at an equatorial distance $\approx$ 11 Re, is characterized by a steep electron pressure gradient, with a length scale of $\approx$ 0.4 Re, as well as a steep temperature gradient (to use the work "temperature"

loosely to refer to the energy of the peak of the spectrum) but only a weak density gradient. During bay activity the boundary, now located at $\approx$ 6 Re, is still characterized by the same electron pressure gradient, with a only slightly longer length scale of $\approx$ 0.6 Re, but now there is a more complicated density and temperature structure: within the "boundary layer" defined by the pressure gradient, the temperature first decreases and then increases again while the density behaves in the opposite way; then the temperature decreases again, dropping below the energy range of the OGO-1 detector, while the density appears to remain constant or to decrease slightly.

Acknowledgements. — I acknowledge with pleasure numerous discussions with my colleagues at M.I.T., particularly Prof. H. S. Bridge, Prof. S. Olbert, Prof. G. L. Siscoe, Dr. J. H. Binsack, and Prof. A. J. Lazarus. I am grateful to Dr. J. P. Heppner and his co-workers at Goddard Space Flight Center for exchange of information and discussions regarding OGO-1 magnetometer data as well as auroral zone phenomena.

This research was supported in part by the National Aeronautics and Space Administration under contract NAS 5-2053 and grant NsG-386, and in part by the Atomic Energy Commission under contract AT(30-1)-2098.

References

Angerami, J. J., and D. L. Carpenter, Whistler studies of the plasmapause in the magnetosphere, 2, Electron density and total tube electron content near the knee in magnetospheric ionization, J. Geophys. Res., 71, 711-725, 1966.

Axford, W. I., H. E. Petschek, and G. L. Siscoe, Tail of the magnetosphere, J. Geophys. Res., 70, 1231-1236, 1965.

Axford, W. I., Magnetic storm effects associated with the tail of the magnetosphere, to be published in Proceedings of the ESRO Conference on the Magnetosphere held in Stockholm, November 1965; also Cornell-Sydney University Astronomy Center report CSUAC 32, 1966.

Bame, S. J., J. R. Asbridge, H. E. Felthauser, R. A. Olson, and I. B. Strong, Electrons in the plasma sheet of the earth's magnetic tail, Phys. Rev. Letters, 16, 138-142, 1966.

Bame, S. J., J. R. Asbridge, H. E. Felthauser, E. W. Hones, and I. B. Strong, Characteristics of the plasma sheet in the earth's magnetotail, J. Geophys. Res., 72, 113-129, 1967.

Binsack, J. H., Plasmapause observations with the M.I.T. experiment on IMP-2, J. Geophys. Res., 72, (21), 1967.

Carpenter, D. L., Whistler studies of the plasmapause in the magnetosphere, 1, Temporal variations in the position of the knee and some evidence on plasma motions near the knee, J. Geophys. Res., 71, 693-709, 1966.

Cladis, J. B., Motion of geomagnetic flux tube resulting from injection of hot plasma (abstract), Trans. A.G.U., 48, 157, 1967.

Dessler, A. J., and R. D. Juday, Configuration of auroral radiation in space, Planetary Space Sci., 13, 63-72, 1965.

Frank, L. A., A survey of electrons > 40 kev beyond 5 earth radii with Explorer 14, J. Geophys. Res., 70, 1593-1626, 1965.

Gringauz, K. I., V. G. Kurt, V. I. Moroz, and I. S. Shklovskii, Results of observations of charged particles observed out to R = 100,000 km with the aid of charged-particle traps on Soviet space rockets, Astron. Zh., 37, 716-735, 1960 (English translation: Soviet Astron. AJ, 4, 680-695, 1961).

Gringauz, K. I., V. V. Bezrukikh, L. S. Musatov, R. E. Rybchinsky, and S. M. Sheronova, Measurements made in the earth's magnetosphere by means of charged particle traps aboard the Mars 1 probe, Space Res., IV, edited by P. Muller, pp. 621-626, North-Holland Publishing Company, Amsterdam, 1964.

Heppner, J. P., Recent measurements of the magnetic field in the outer magnetosphere and boundary regions, paper presented at ESRO Colloquium on Auroral and Associated Magnetospheric Phenomena at Very High Latitudes, Stockholm, Sweden, November 1965; Goddard Space Flight Center report X-612-65-490, 1965.

Heppner, J. P., M. Sugiura, T. L. Skillman, B. G. Ledley, and M. Campbell, OGO-A Magnetic field observations, GSFC Report X-612-67-150, March 1967.

Ness, N. F., The earth's magnetic tail, J. Geophys. Res., 70, 2989-3003, 1965.

Serlemitsos, P., Low-energy electrons in the dark magnetosphere, J. Geophys. Res., 71, 61-77, 1966.

Sugiura, M., and J. P. Heppner, The earth's magnetic field, in Introduction to Space Science, edited by W. Hess, pp. 5-92, Gordon and Breach, New York, 1965.

Taylor, H. A., Jr., H. C. Brinton, and C. R. Smith, Positive ion composition in the magnetoionosphere obtained from the Ogo-A satellite, J. Geophys. Res., 70, 5769-5781, 1965.

Vasyliunas, V. M., Observations of 50-to 2000-ev electrons with OGO-A (abstract), Trans. A.G.U., 47, 142, 1966; Observations of low energy electrons with the OGO-A satellite, Ph.D. thesis, M.I.T., 1966.

Vasyliunas, V. M., A survey of low energy electrons in the evening sector of the magnetosphere with OGO-1 and OGO-3, to be published, 1968.

Figure Captions

Figure 1. Equatorial cut of the magnetosphere, showing the principal features of the low energy electron population as established by various satellites.

Figure 2. Meridian cut of the magnetosphere, along the line CC' of Figure 1.

Figure 3. OGO-1 data for a typical inbound pass near the dusk meridian. The four curves are the currents measured in the four energy channels of the detector; the ordinate is an approximately logarithmic representation of the current, one division being a factor of ≈ 3. The energy bandpasses of channels 1 to 4 are, roughly, 550-1800 ev, 320-1000, 180-550, 126-350 (see Vasyliunas, 1968 for a detailed description of the detector response). "S-E-P" is the sun-earth-satellite (probe) angle; "azimuth" is the angle of the satellite above the ecliptic, projected on a plane normal to the sun-earth line. M indicates the approximate position of the magnetopause.

Figure 4. Meridian plane projection of the OGO-1 orbit corresponding to Figure 3. Dashed line: geomagnetic coordinates. Solid line: solar magnetospheric coordinates (as defined by Ness, 1965).

Figure 5. A "map" of the OGO-1 observations, projected on the solar magnetospheric equatorial plane (X axis toward the sun; Y axis normal to the earth's dipole and the sun-earth line, pointing toward the dusk side). See text for explanation.

Figure 6. Radial distances of observed crossings of the plasma sheet inner boundary, plotted against magnetic local time. Presence or absence of bay activity at time of crossing is indicated.

Figure 7. OGO-1 electron data and auroral zone magnetograms for the October 11-12, 1964 inbound pass.

Figure 8. Same as Figure 7, for October 14, 1964.

Figure 9. Same as Figure 7, for October 17, 1964.

Figure 10. Sketch of changes in the spatial distribution of low energy electrons during magnetic bays.

Figure 11. Same as Figure 5 but omitting observations during periods of bay activity.

Figure 12. Variation of electron spectral parameters across the inner boundary for the November 5, 1964 inbound pass.

Figure 13. Currents measured in channels 1 and 4 as functions of radial distance for a number of inner boundary crossings. The ordinate is the same as in Figure 3 but with origin shifted to the background level.

Figure 14. Same as Figure 12, for October 17, 1964.

Figure 15. Same as Figure 12, for October 1, 1964.

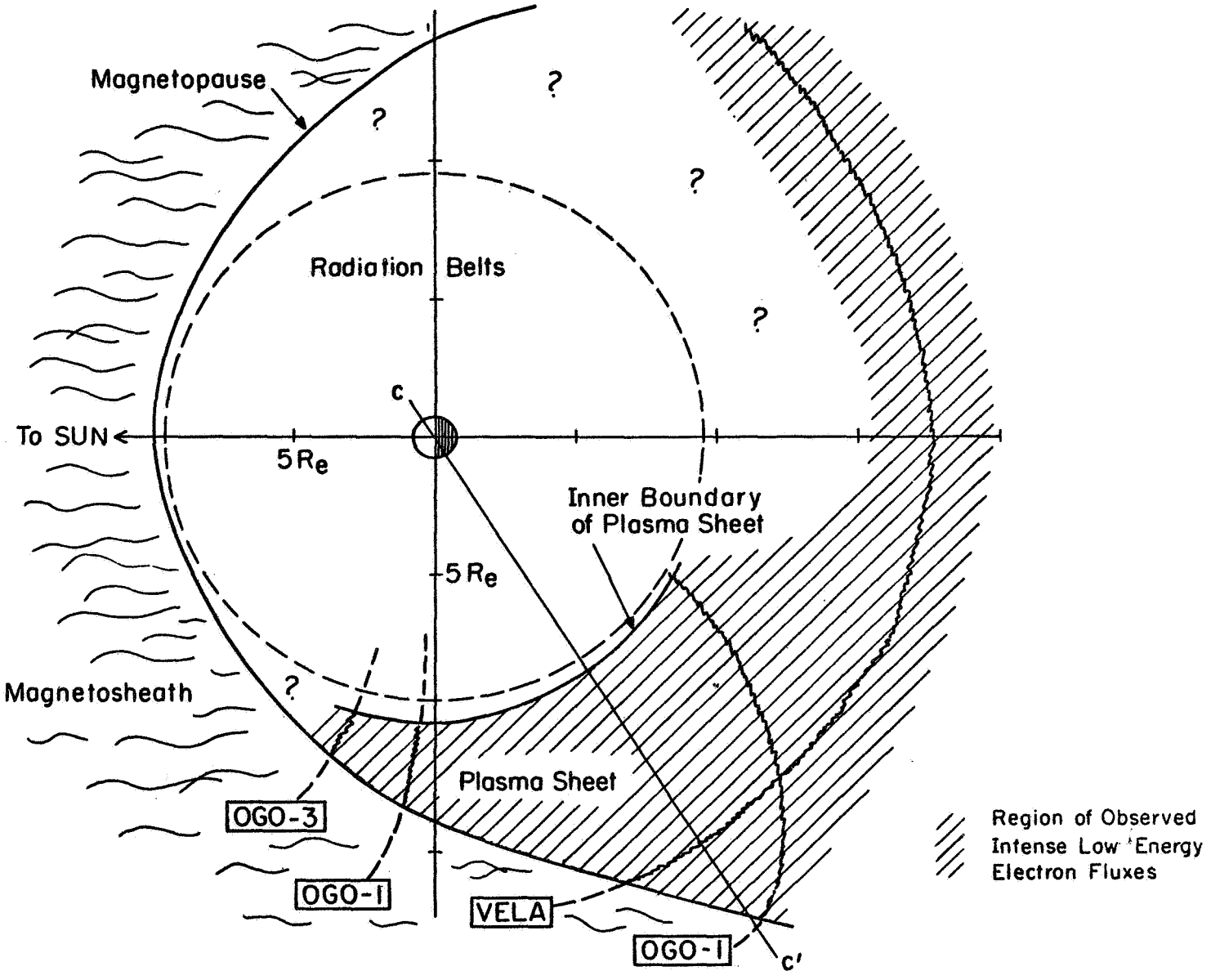

DISTRIBUTION OF LOW ENERGY (~100 - 1000eV) ELECTRONS
IN THE EQUATORIAL REGION OF THE MAGNETOSPHERE
(Viewed from above the North Pole)

Figure 1

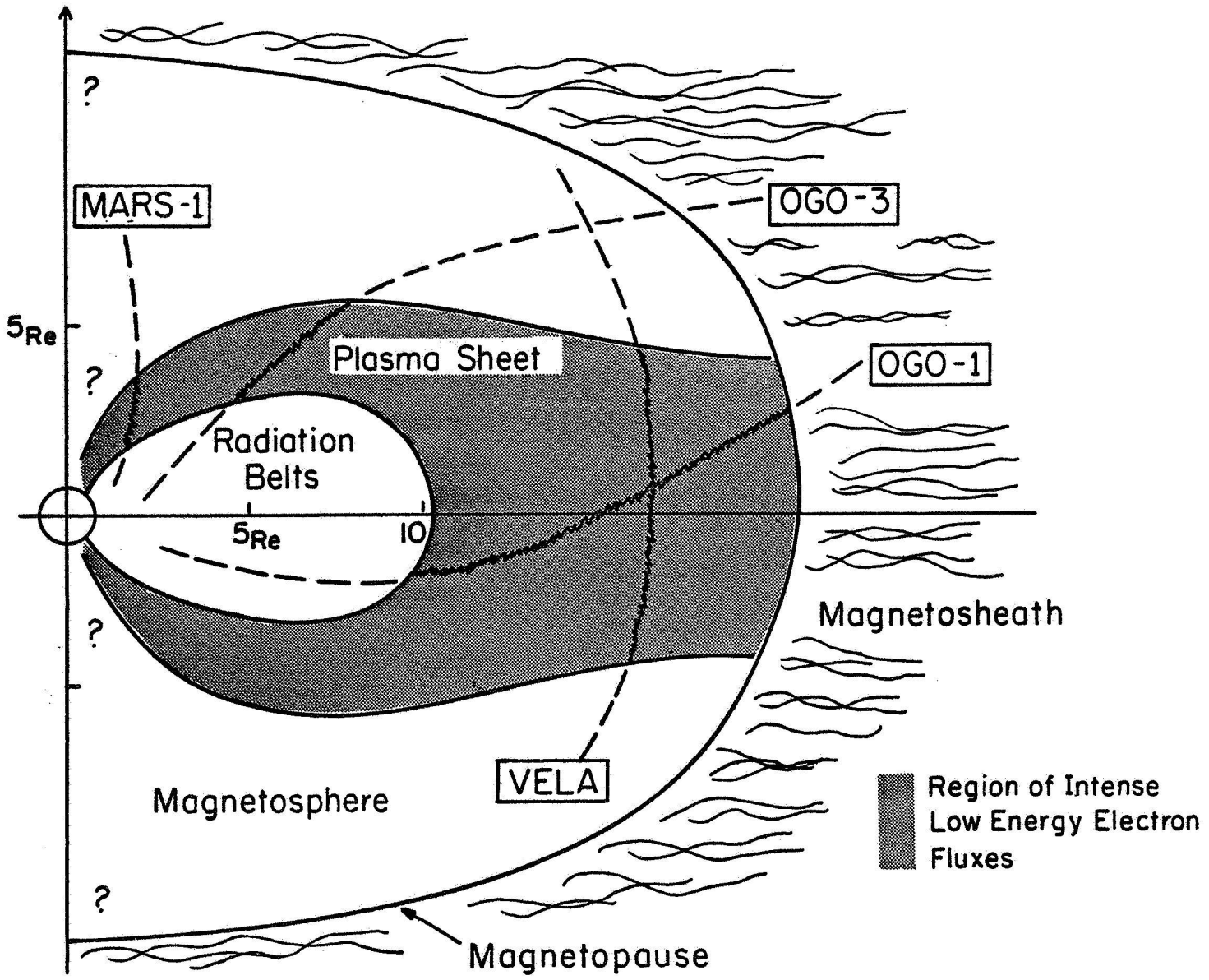

DISTRIBUTION OF LOW ENERGY (~100-1000 eV)
ELECTRONS IN THE MAGNETOSPHERE
(Viewed in a late evening meridian plane)

Figure 2

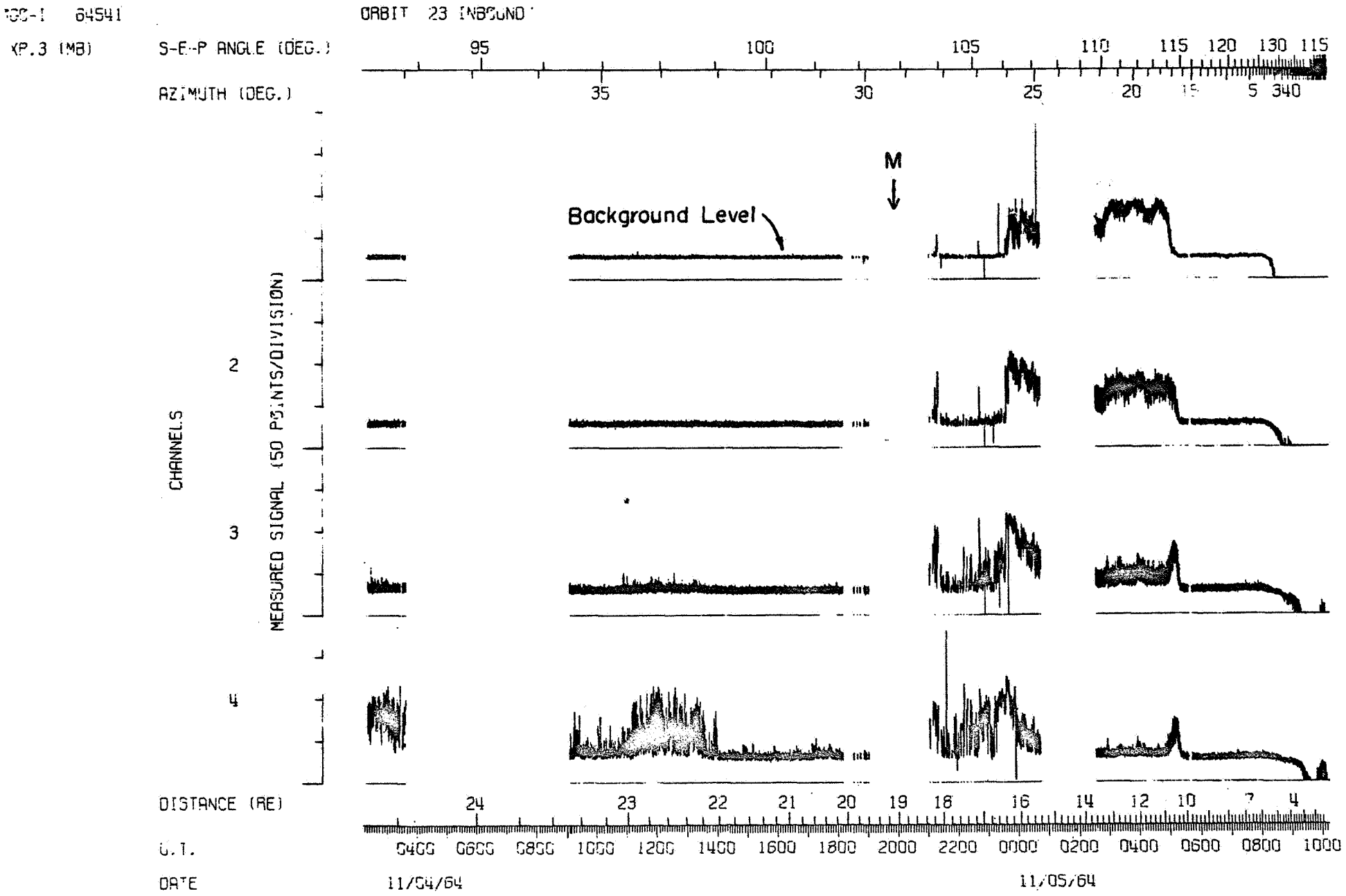
OGO-I 64541
ORBIT 23 INBOUND
XP.3 (MB)
S-E-P ANGLE (DEG.)
95 100 105 110 115 120 130 115
AZIMUTH (DEG.)
35 30 25 20 5 340
M
Background Level
CHANNELS
2
3
4
MEASURED SIGNAL (50 POINTS/DIVISION)
DISTANCE (RE)
24 23 22 21 20 19 18 16 14 12 10 7 4
U.T.
0400 0600 0800 1000 1200 1400 1600 1800 2000 2200 0000 0200 0400 0600 0800 1000
DATE
11/04/64
11/05/64

Figure 3

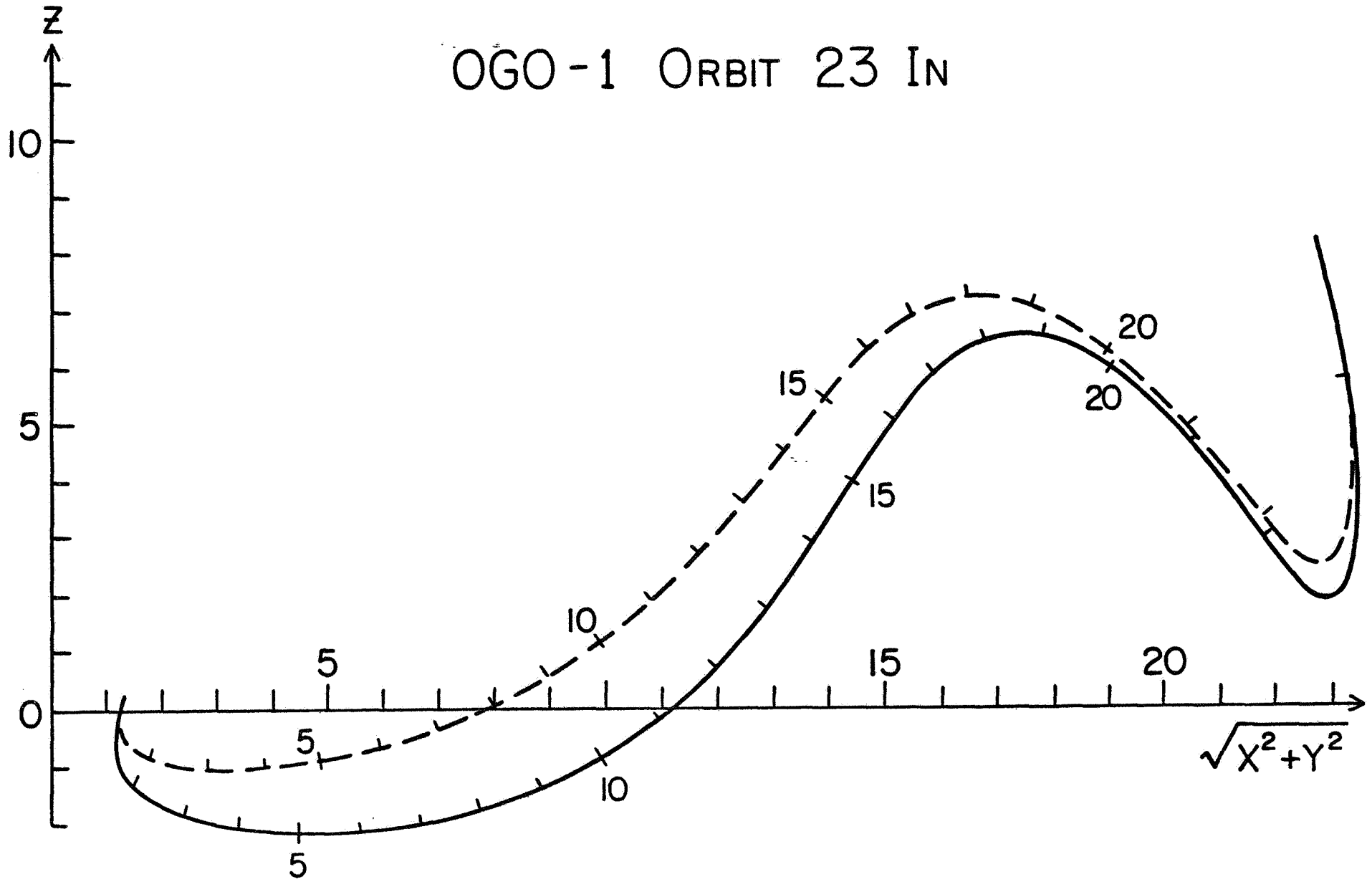

Figure 4

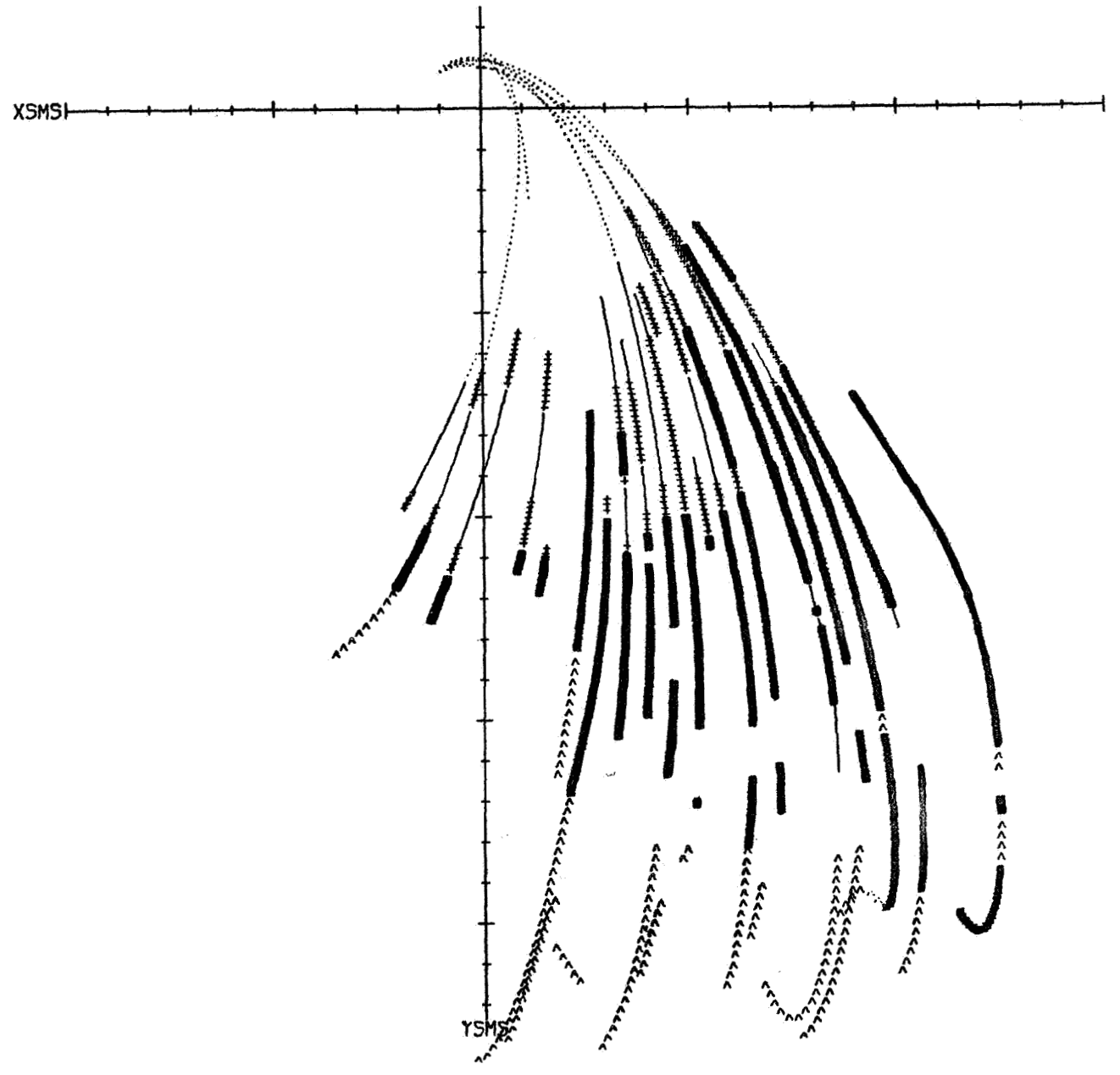

STRONG FLUX, PLASMA SHEET

WEAK FLUX, ON THE EARTHWARD SIDE OF THE INNER BOUNDARY

NO DETECTABLE FLUX

MAGNETOSHEATH

PLASMASPHERE

Figure 5

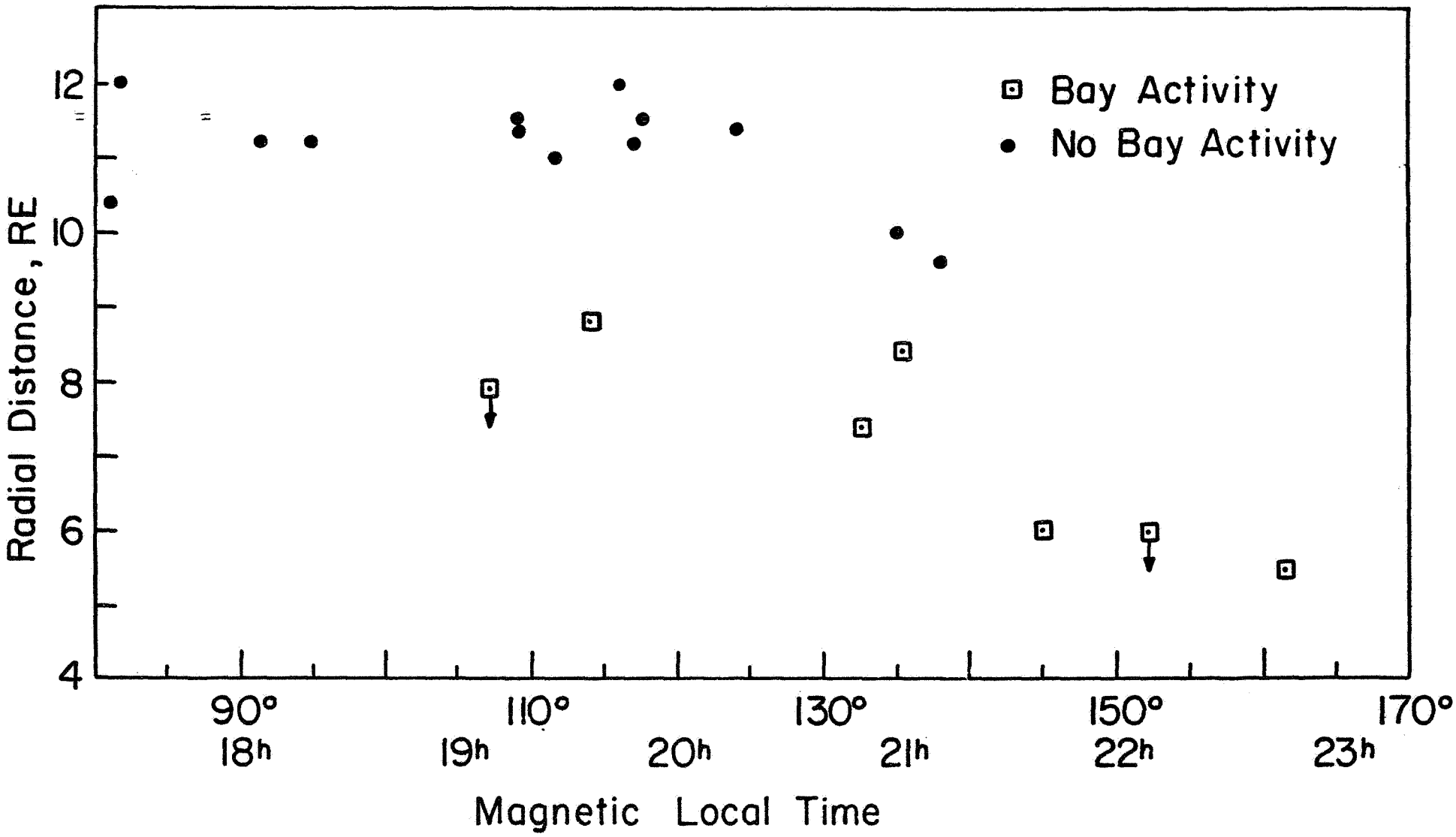
Bay Activity
No Bay Activity
Radial Distance, RE
12
10
8
6
4
90°
110°
130°
150°
170°
18h
19h
20h
21h
22h
23h
Magnetic Local Time

Figure 6

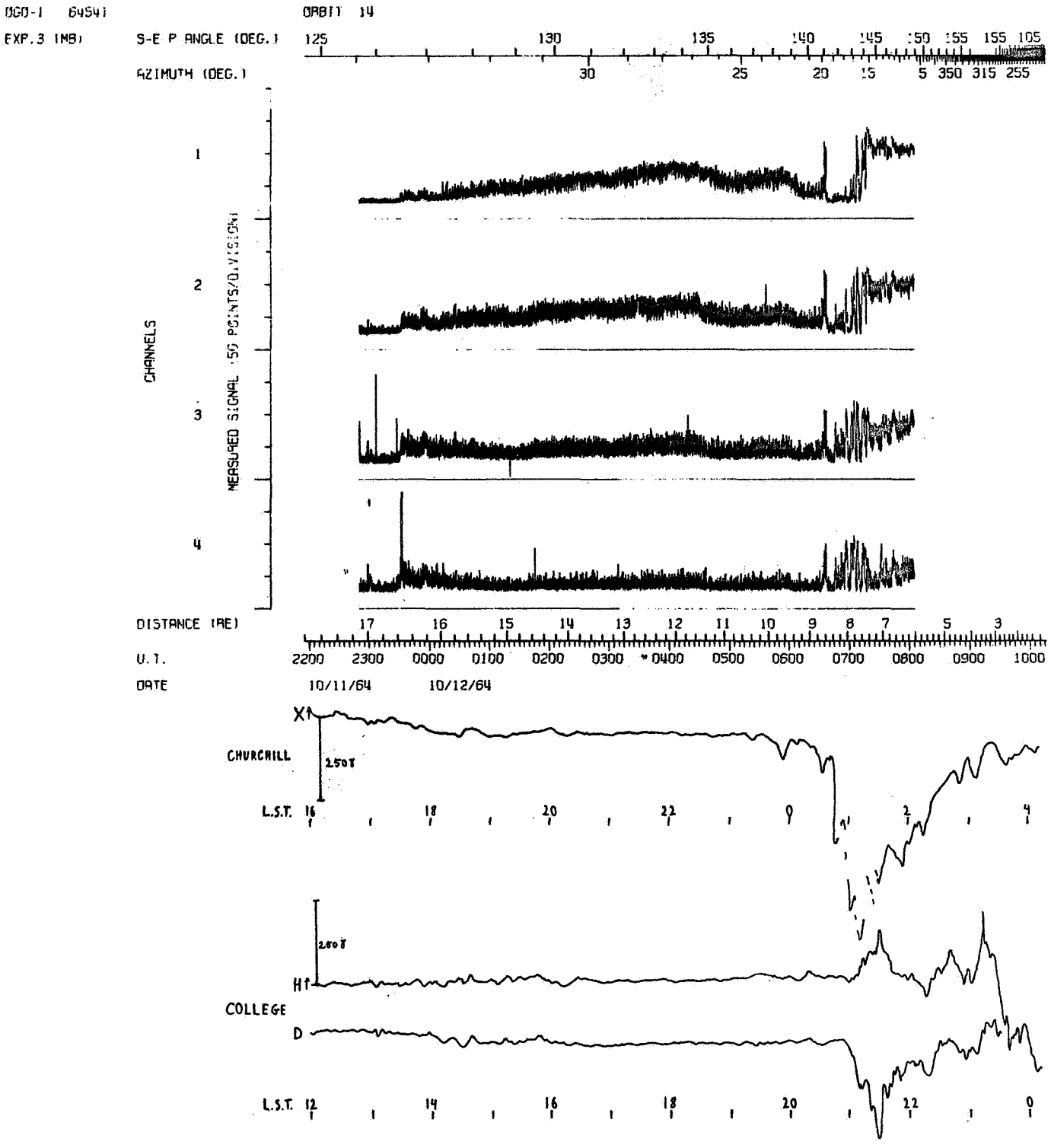
OGO-I 6454
EXP.3 (MB)
ORBIT 14
S-E P ANGLE (DEG.)
125 130 135 140 145 150 155 155 105
AZIMUTH (DEG.)
30 25 20 15 5 350 315 255
CHANNELS
MEASURED SIGNAL 50 POINTS/DIVISION
1
2
3
4
DISTANCE (RE)
17 16 15 14 13 12 11 10 9 8 7 5 3
U.T.
2200 2300 0000 0100 0200 0300 0400 0500 0600 0700 0800 0900 1000
DATE
10/11/64 10/12/64
X
CHURCHILL
250γ
L.S.T. 16 18 20 22 0 2 4
250γ
H
COLLEGE
D
L.S.T. 12 14 16 18 20 22 0

Figure 7

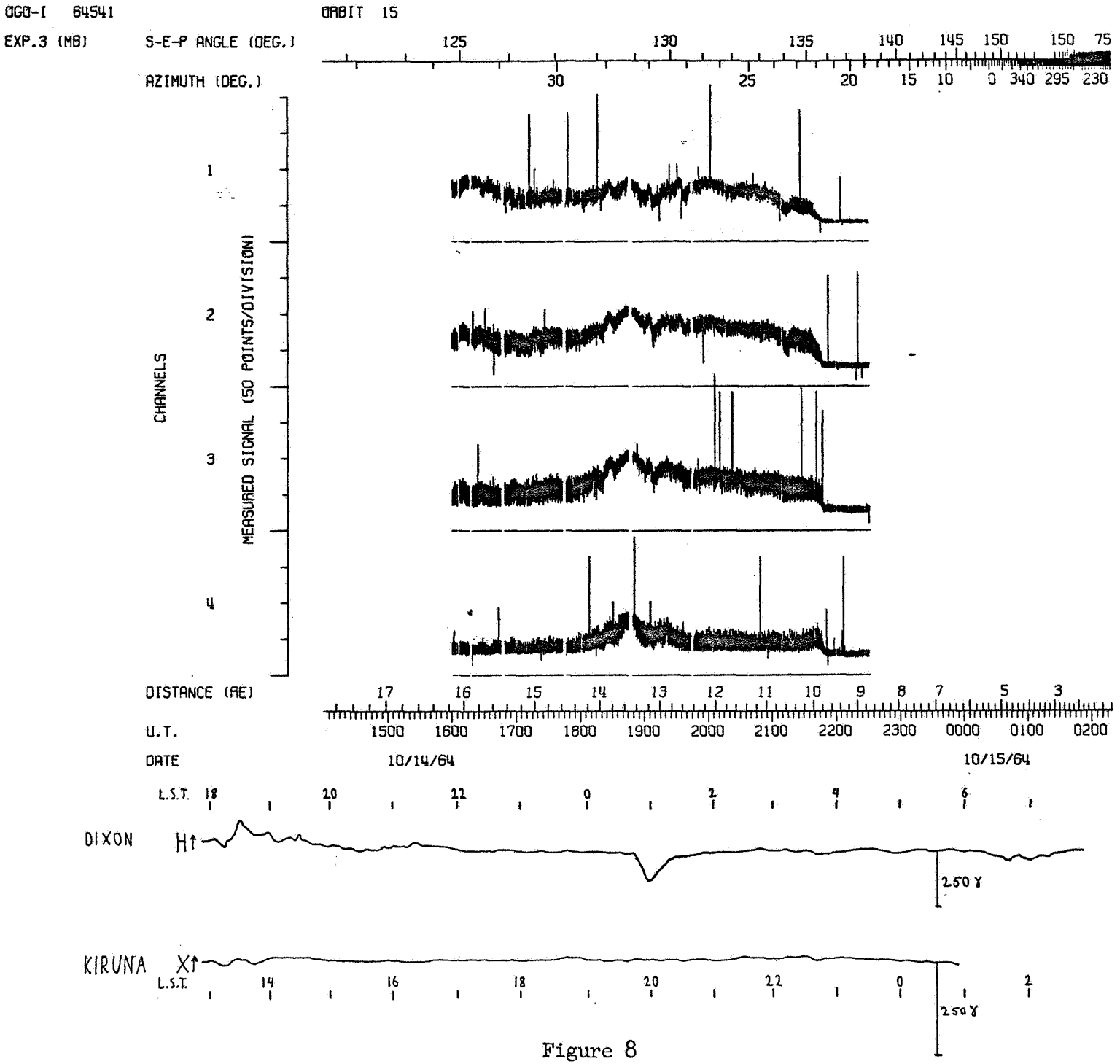
OGO-I 64541
ORBIT 15
EXP.3 (MB)
S-E-P ANGLE (DEG.)
125 130 135 140 145 150 150 75
AZIMUTH (DEG.)
30 25 20 15 10 0 340 295 230
CHANNELS
MEASURED SIGNAL (50 POINTS/DIVISION)
1
2
3
4
DISTANCE (RE)
17 16 15 14 13 12 11 10 9 8 7 5 3
U.T.
1500 1600 1700 1800 1900 2000 2100 2200 2300 0000 0100 0200
DATE
10/14/64
10/15/64
L.S.T. 18 20 22 0 2 4 6
DIXON H↑
250 γ
KIRUNA X↑
L.S.T. 14 16 18 20 22 0 2
250 γ

Figure 8

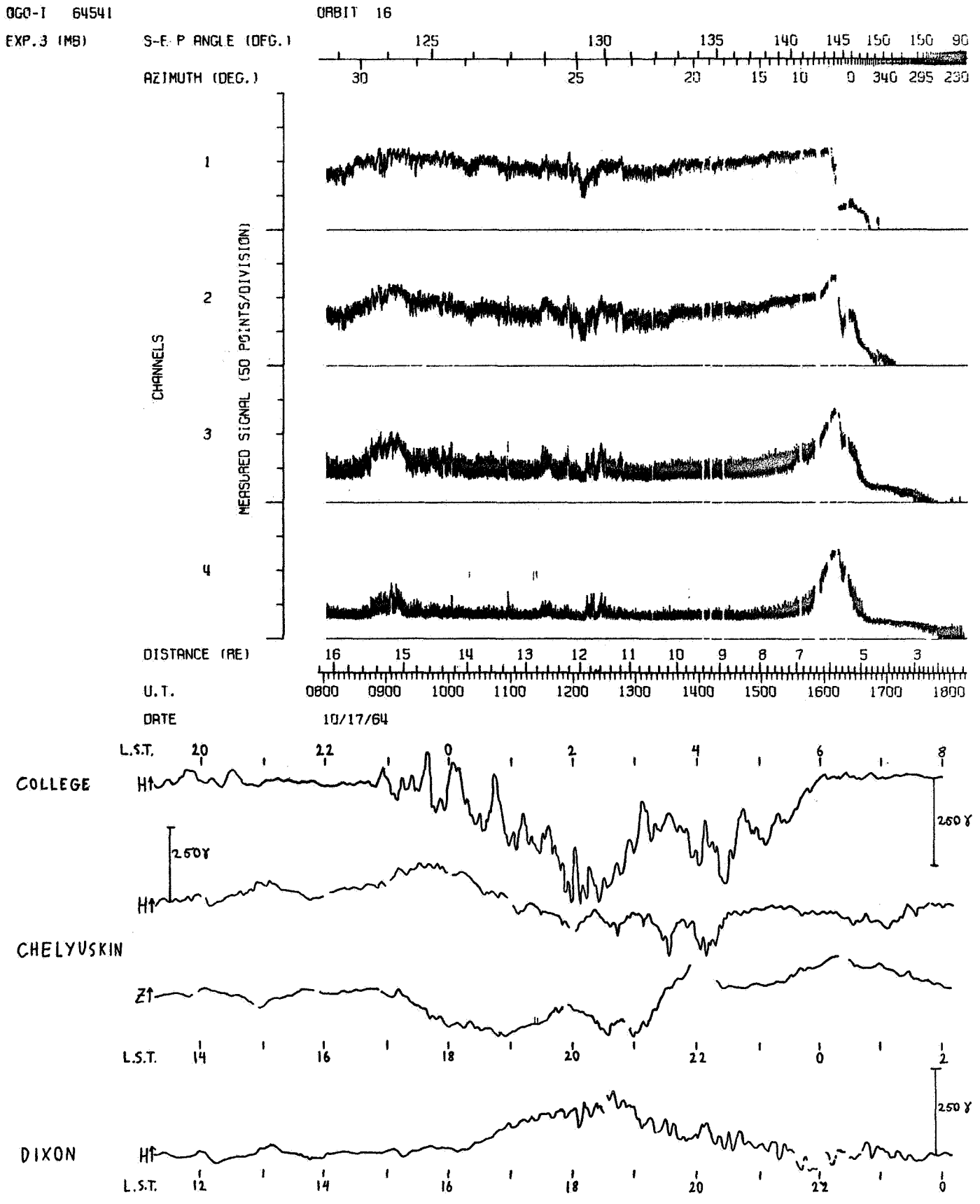
OGO-I 64541
EXP.3 (MB)
ORBIT 16
S-E P ANGLE (DEG.)
125 130 135 140 145 150 150 90
AZIMUTH (DEG.)
30 25 20 15 10 0 340 295 230
CHANNELS
MEASURED SIGNAL (50 POINTS/DIVISION)
1
2
3
4
DISTANCE (RE)
16 15 14 13 12 11 10 9 8 7 5 3
U.T.
0800 0900 1000 1100 1200 1300 1400 1500 1600 1700 1800
DATE
10/17/64
L.S.T.
20 22 0 2 4 6 8
COLLEGE
Ht
260 γ
260 γ
Ht
CHELYUSKIN
Z↑
L.S.T.
14 16 18 20 22 0 2
250 γ
DIXON
Ht
L.S.T.
12 14 16 18 20 22 0

Figure 9

SCHEMATIC PLASMA SHEET CONFIGURATION
(in equatorial plane)

(a) During quiet times

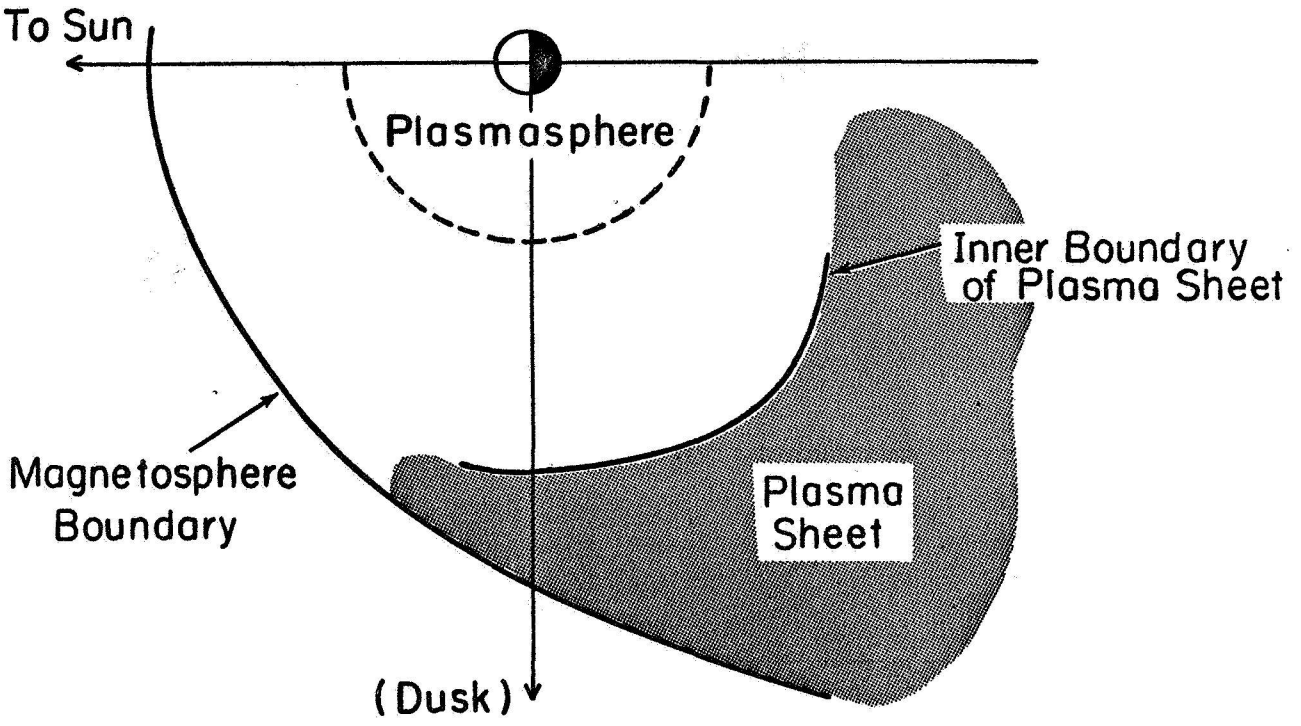

(b) During magnetic bays

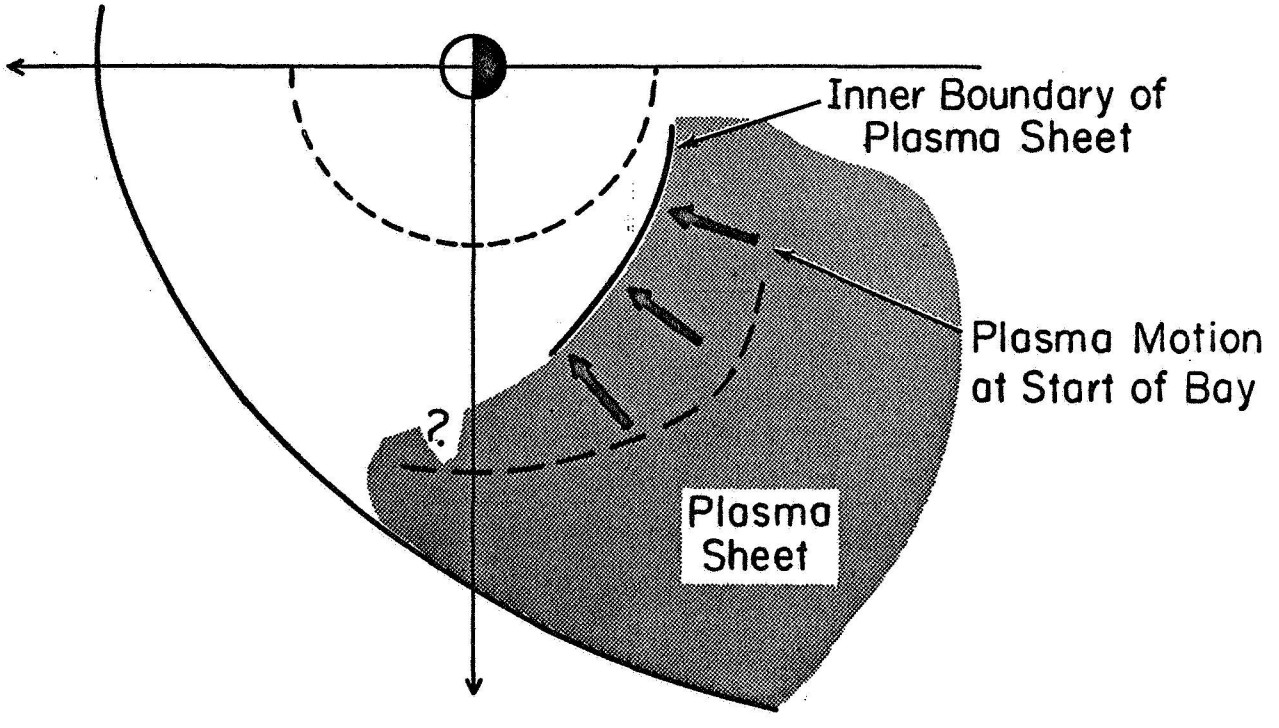

Figure 10

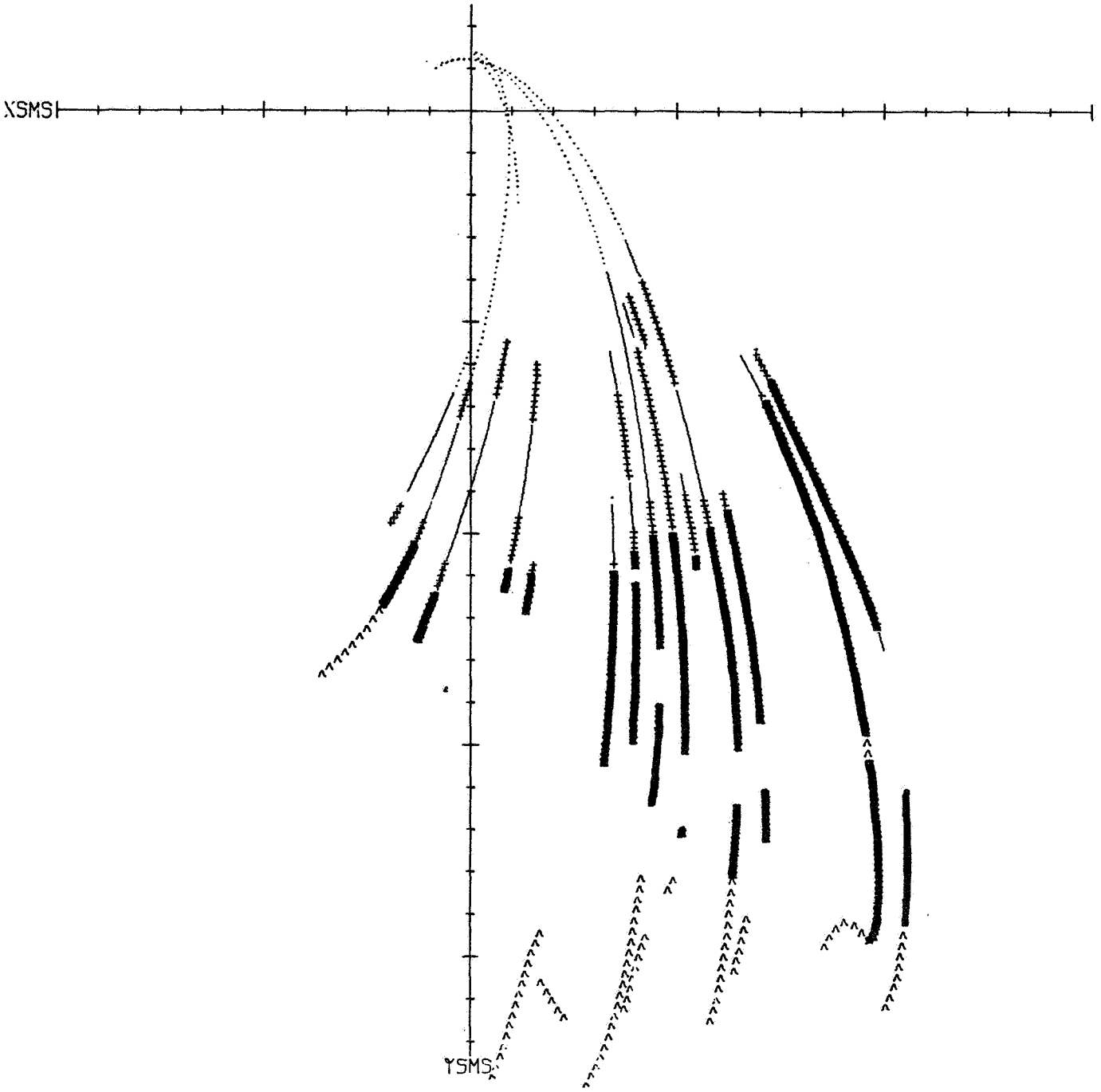

Figure 11

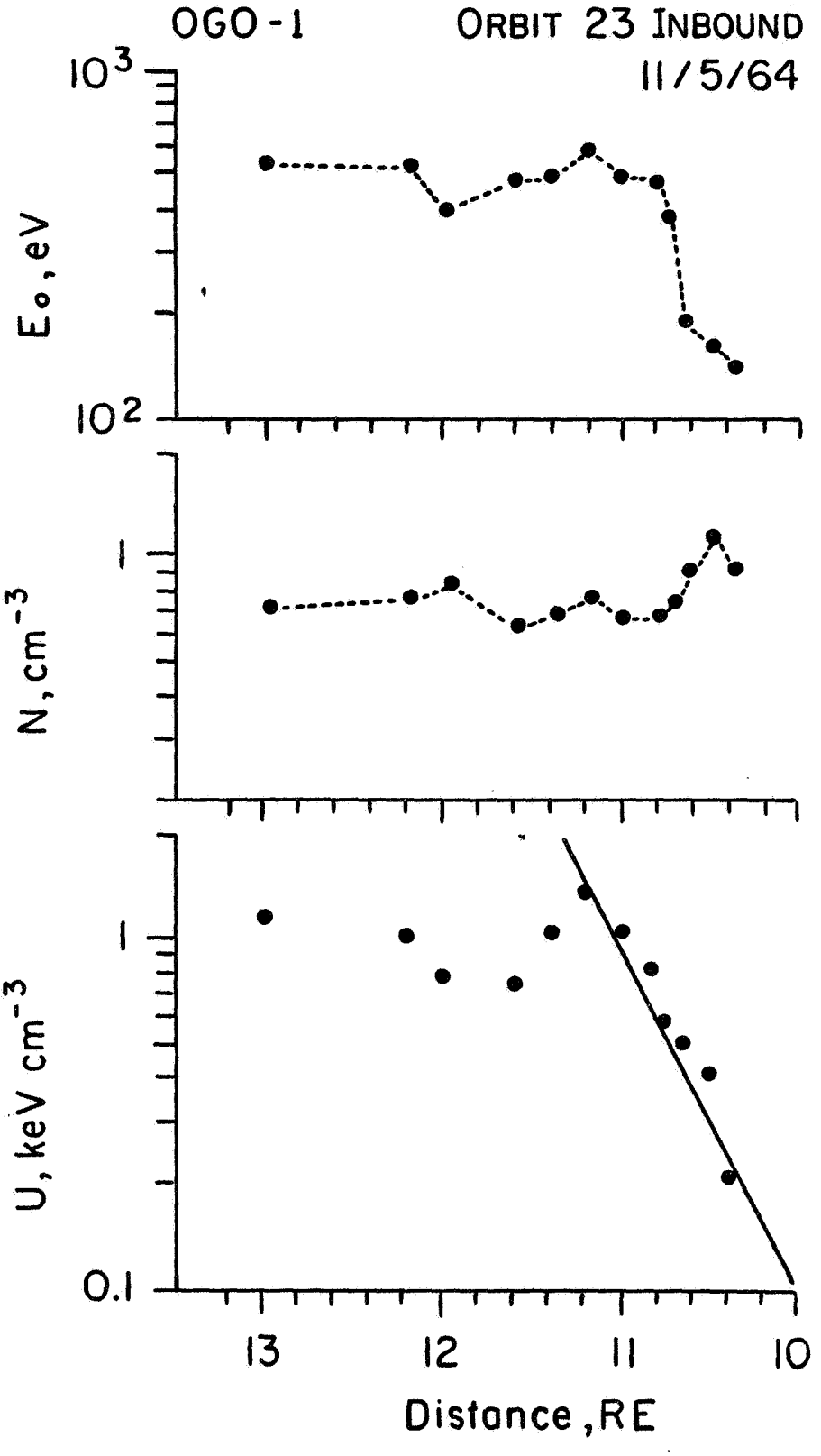
OGO-1
ORBIT 23 INBOUND
11/5/64
10^3
10^2
E_o, eV
1
N, cm^{-3}
1
0.1
U, keV cm^{-3}
13
12
11
10
Distance, RE

Figure 12

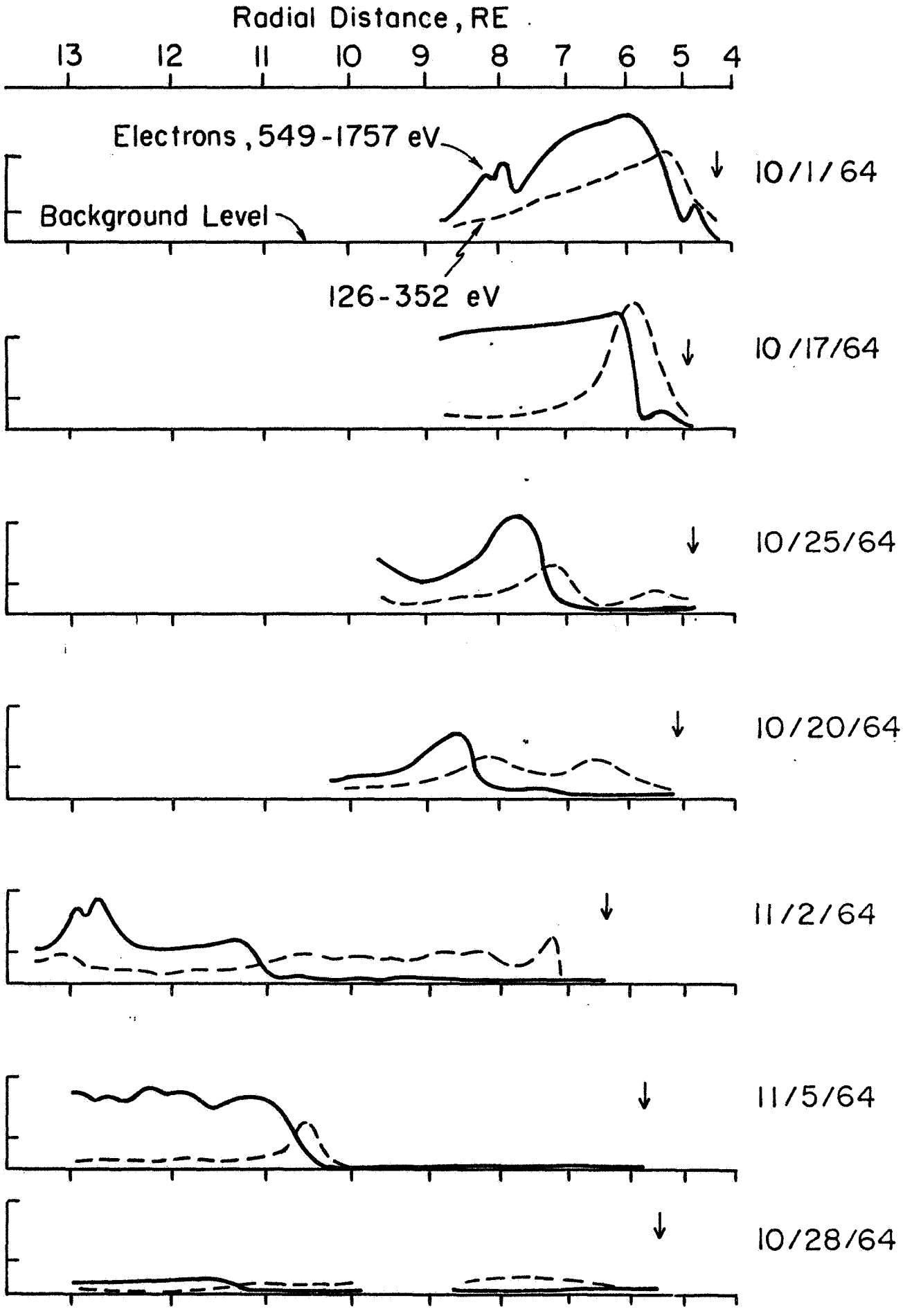
Radial Distance, RE
13
12
11
10
9
8
7
6
5
4
Electrons, 549-1757 eV
Background Level
126-352 eV
10/1/64
10/17/64
10/25/64
10/20/64
11/2/64
11/5/64
10/28/64

Figure 13

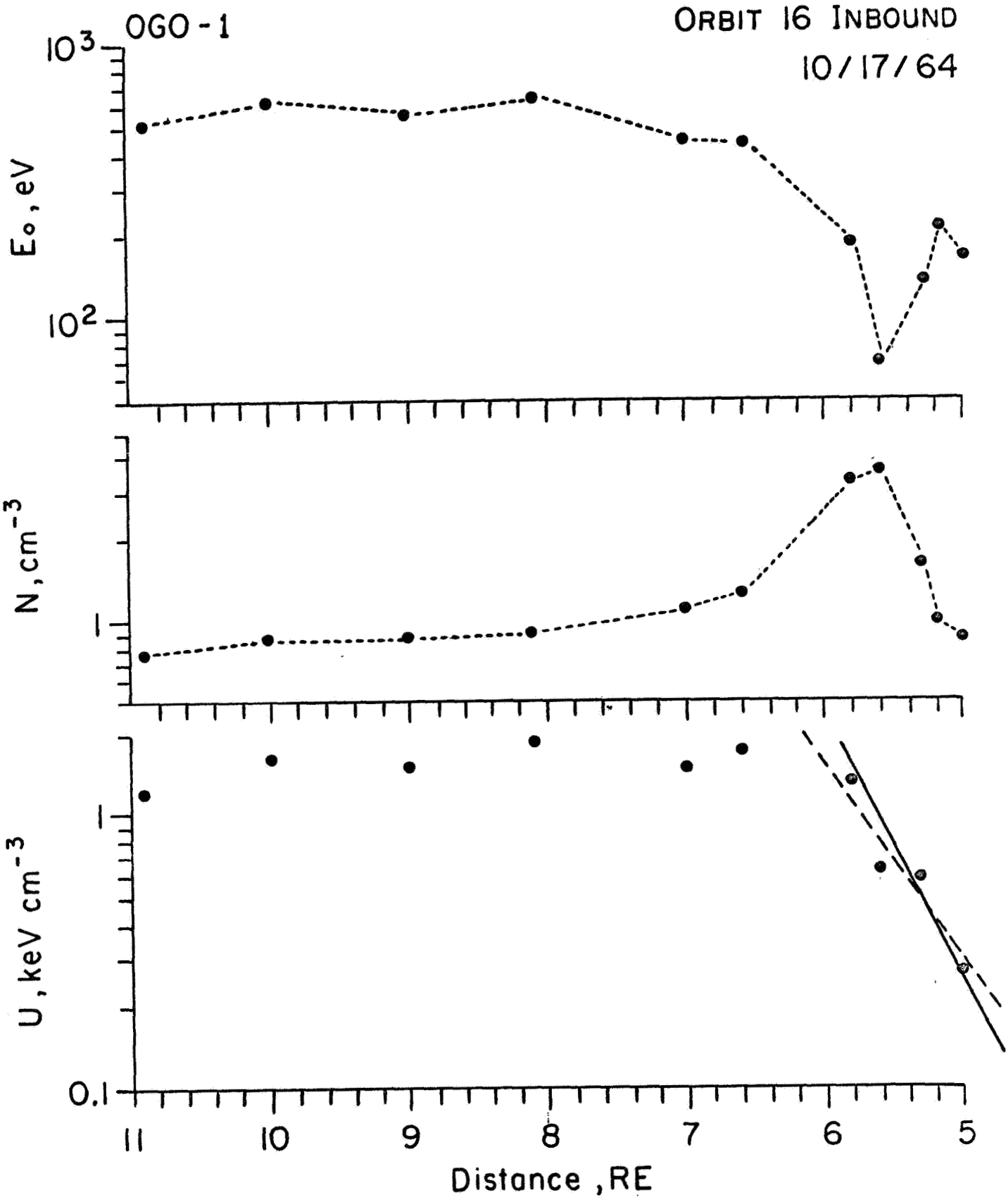
OGO-1
ORBIT 16 INBOUND
10/17/64
10^3
10^2
E_o, eV
N, cm^{-3}
U, keV cm^{-3}
0.1
11
10
9
8
7
6
5
Distance, RE

Figure 14

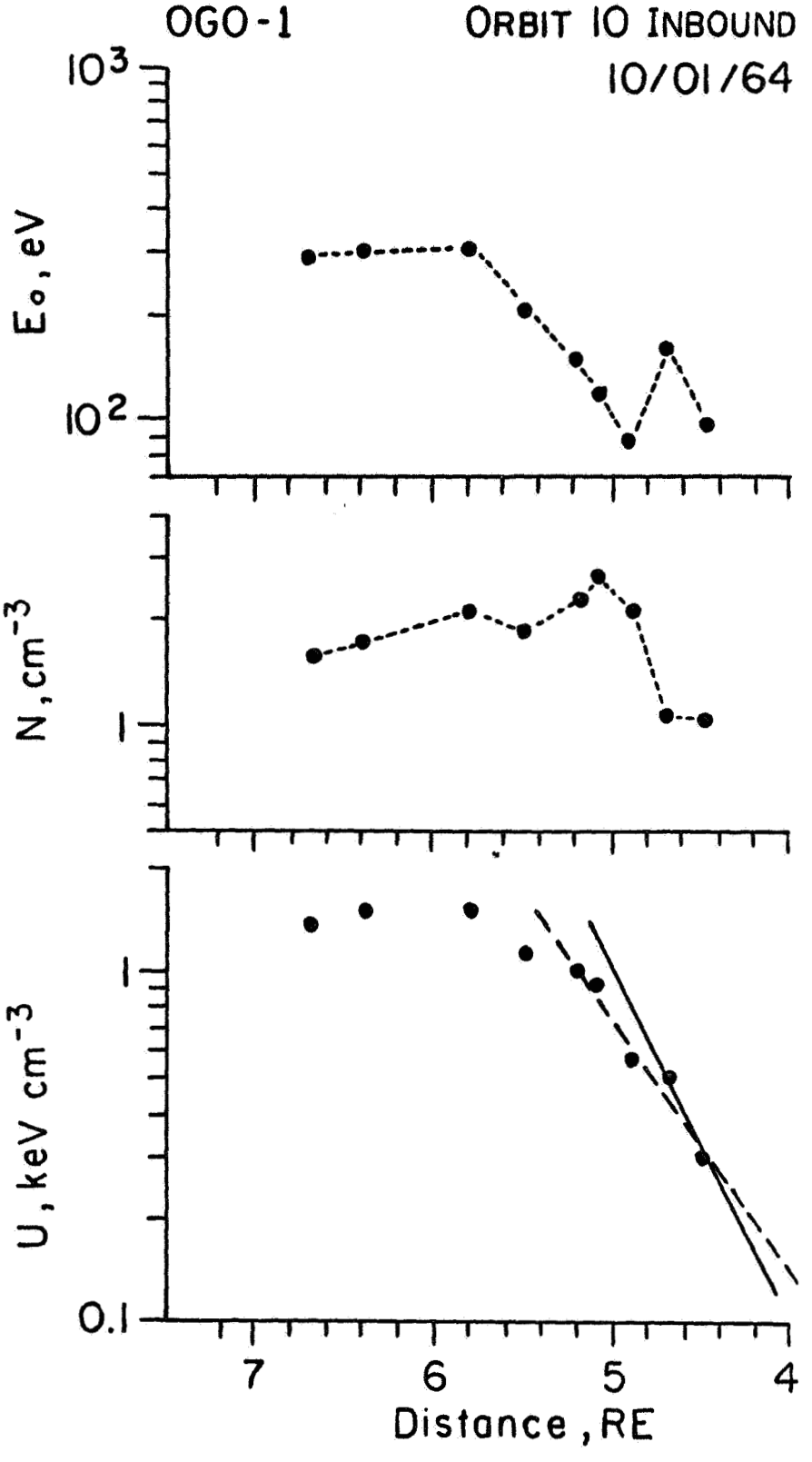
OGO-1
ORBIT 10 INBOUND
10/01/64
10^3
10^2
E_o, eV
N, cm^{-3}
1
U, keV cm^{-3}
1
0.1
7
6
5
4
Distance, RE

Figure 15